WIRELESS COMMUNICATIONS AND MOBILE COMPUTING
Wirel. Commun. Mob. Comput. (2012)
Published online in Wiley Online Library (wileyonlinelibrary.com). DOI: 10.1002/wcm.2330

SPECIAL ISSUE PAPER

Capacity limits in a variable duty cycle IEEE 802.11p-based VANET

Serkan Ozturk[1], Jelena Mišić[2*] and Vojislav B. Mišić[2]

[1] Erciyes University, Kayseri, Turkey
[2] Ryerson University, Toronto, ON, Canada

ABSTRACT

In this paper, we investigate the capacity limits in a variable duty cycle VANET that uses the IEEE 802.11p standard. We show that the default value of duty cycle that allocates time equally between control and service channels leads to unbalanced performance and that the performance of typical traffic on those channels can be greatly improved by judicious choice of the value for duty cycle. We find the values of spatial density of vehicular traffic that lead to spatial saturation of network traffic. In addition, to model the distribution of the vehicles on the road segment, we used Poisson distribution, as well as Erlang-*k* distribution. Copyright © 2012 John Wiley & Sons, Ltd.

KEYWORDS
IEEE 802.11p; performance evaluation; spatial saturation

***Correspondence**
Jelena Mišić, Ryerson University, Toronto, ON, Canada.
E-mail: jmisic@scs.ryerson.ca

1. INTRODUCTION

VANETs are a fast growing segment of networking technology that aims to integrate diverse networking functions and services, including, but not limited to, road safety messages, electronic toll collection, infotainment services, and other intelligent transportation applications, into a flexible and usable system. One of the most popular VANET technologies today is IEEE 802.11p, a dedicated short-range communications (DSRC) standard for wireless access in vehicular environment (WAVE), which uses one central control channel (CCH) and six service channels (SCHs) with a total bandwidth of 75 MHz in the licensed spectrum at 5.9 GHz as shown in Figure 1. Stations utilizing IEEE 802.11p can be mounted on-board the vehicles themselves or on a dedicated stationary roadside structures; they will hereafter be referred to as on-board unit (OBU) and roadside unit (RSU), respectively. In DSRC/WAVE, the CCH is envisioned to carry high-priority traffic safety messages, whereas the SCHs are dedicated to various transportation services, including paid services and infotainment. Both CCH and SCH support four data classes with aggressively differentiated priorities as shown in Tables I and II [1].

Despite the better performance of multi-channel WAVE devices, in most cases, single-channel devices are preferred because of lower cost; in this case, an OBU device can utilize only one channel at a time, which implies switching between CCH and SCHs during each sync interval, as shown in Figure 2. The performance of the network is, then, very much dependent on the duty cycle, that is, the ratio of the time allocated to CCH and SCH with respect to the total duration of the sync interval. As is well known, CCH traffic is needed to fulfill the safety purpose of a VANET, whereas SCH traffic can bring in the revenue needed to actually design, build, and deploy the necessary VANET infrastructure. As a result, some trade-off between the performance on the two channels is desirable. Our earlier work [2,3] has indicated that the default value of the duty cycle—the time division between CCH and SCHs—leads to unbalanced performance. Therefore, this paper aims to investigate whether varying the duty cycle will allow a more balanced performance in the case of an RSU operating on a bidirectional road segment for different transmission ranges.

Distribution of vehicles on road section is important for VANET. In this work, we used Poisson and discrete version of Erlang-*k* distributions for modeling the distribution of the vehicles on the road segment. We combine vehicular traffic theory, M/G/1 queuing analysis, and Markov chain analysis partly used in our previous work [3] in order to investigate the effect of duty cycle for an IEEE 802.11p-based network. Assuming error-prone channel conditions,

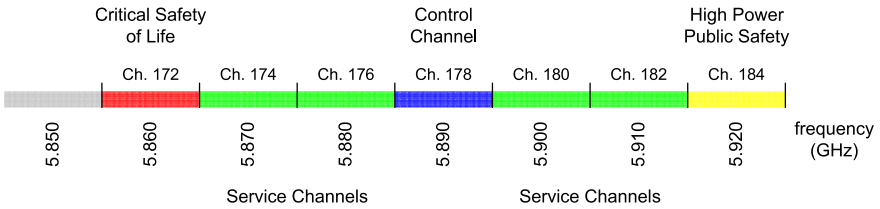

Figure 1. WAVE channels.

Table I. EDCA parameter set used on the control channel (adapted from [1]).

ACI	AC	CWmin	CWmax	AIFSN
1	Background	15	511	9
0	Best effort	7	15	6
2	Video	3	7	3
3	Voice	3	7	2

EDCA, Enhanced Distributed Channel Access; AC, access category; ACI, access category index; AIFS, arbitration inter-frame space; AIFSN, AIFS Number; CW, contention window.

Table II. EDCA parameter set used on the service channel (adapted from [1]).

ACI	AC	CWmin	CWmax	AIFSN
1	Background	15	511	7
0	Best effort	15	511	3
2	Video	7	15	2
3	Voice	3	7	2

EDCA, Enhanced Distributed Channel Access; AC, access category; ACI, access category index; AIFS, arbitration inter-frame space; AIFSN, AIFS Number; CW, contention window.

we derive probability distributions for frame backoff time, waiting time in queue, and collision probability of a transmission for each channel and each data class within that particular data combination. In this study, we also compared the effect of distributions of Poisson and Erlang-k in our model.

The remainder of the paper is organized as follows: Section 2 presents some important related work in this area, followed by the basic outline of our analytical model in Section 3. Section 4 presents the numerical results and our findings. Finally, Section 5 concludes the paper.

2. RELATED WORK

The problem of traffic performance has attracted much attention from both academic and industrial perspectives. The capacity of an IEEE 802.11p network was soon found to be very dependent on a number of parameters, including RSU and OBU transmission ranges, vehicle density and mobility, and traffic parameters such as traffic volume (expressed via the packet arrival rate) and the distribution of traffic among the four available classes.

Some authors have combined an IEEE 802.11 model of saturated traffic with free-flow vehicular traffic regime [4] and a Poisson distribution of vehicles in the spatial domain. An analytical model has been proposed in [5] with the goal of quantifying the impact of parameters such as road traffic density and vehicle speed on the download performance of moving vehicles in drive-thru Internet systems. Another analytical framework aimed to evaluate the upload performance for drive-thru Internet as a function of vehicle density [6]. Others have considered heterogeneous vehicular environments where vehicles may have different mobility characteristics [7]. An analytical model to evaluate the medium access control throughput under different node speeds in drive-thru Internet system has been proposed in [8]. A comprehensive analysis of performances of typical headway distribution models is presented in [9]. In their study, to calibrate and examine the performance of various headway models, a large amount of accurate headway observations were obtained.

However, none of the proposed models have considered non-saturation regime, which is much more relevant in practice, for obvious reasons. Our own work in [2] has focused on the transition between saturation and non-saturation modes. We have shown that an increase in vehicle density can result in saturation of the wireless medium in the vicinity and that, in typical scenarios, strong prioritization of traffic leads to virtual victimization of the lowest priority data. Although spatial saturation of vehicles cannot be avoided during rush hour or in the in the vicinity of an accident site, networking saturation can still be avoided by proper dimensioning of resources.

The extension of this work [3] has investigated the impact of different transmission range of the RSU and the

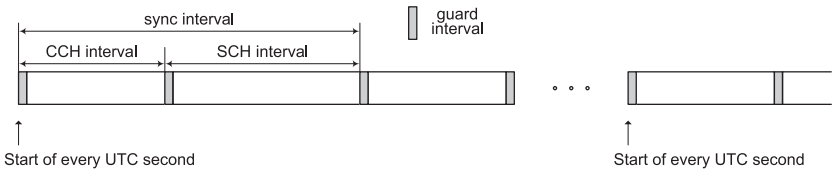

Figure 2. Control channel (CCH)/service channel (SCH) timing. UTC, coordinated universal time.

inter-vehicle distance in a multi-lane highway scenario. Somewhat unexpectedly, we have found that the increase of the transmission range of an RSU does not lead to performance improvement. Instead, it leads to earlier onset of saturation as a result of the large number of vehicles that are serviced by a single RSU. Again, strong prioritization imposed by the IEEE 802.11p standard leads to imbalanced performance between different traffic classes.

3. ANALYTICAL MODEL

In this work, we consider the neighborhood of a single RSU operating in a non-saturation regime deployed on a bidirectional road segment as shown in Figure 3. According to the location to RSU, the road segment is divided into multiple regions [3]. In each region (Rg_i) within the RSU coverage area, vehicles have different payload transmission rates according to their distance to the RSU. Also, we consider OBU devices equipped with a single networking interface only. Each vehicle can transmit frames from data classes AC_k, $k = 0, \ldots, 3$, in either channel, CCH or SCH. Packets from data class k in channel x arrive to the node according to a Poisson process with rate $\lambda_{x,k}$. Time unit in our model is one backoff slot. For data class k within channel x at each region (Rg_r), we assume variable frame size of $ld_{x,k,r}$ slots, which includes payload, medium access control header, and physical header. The probability generating function (PGF) for frame size within the transmission range L of the RSU is

$$Ld_{x,k}(z) = \sum_{r=1}^{Rg_{\max}} \frac{l_r}{L} z^{ld_{x,k,r}} \tag{1}$$

where l_r is the length of the region Rg_r. Duration of the Short Interframe Space (SIFS) period in slots will be denoted as *sifs*. We assume that request-to-send (RTS)/clear-to-send (CTS) transmission scheme is used. Duration of RTS, CTS, and ACK frames expressed in slots will be denoted as *rts*, *cts*, and *ack*, respectively. We model the channel errors through bit error rate (ber). In each region, the probability that frame will not experience noise error is denoted as follows: $\delta_{k,r} = (1 - ber)^{rts_b + cts_b + ld_{b,x,k,r} + ack_b}$ where subscript b denotes values expressed in bits. We assume that node's buffer has infinite length and use $M/G/1$ queuing model. The PGF for successful packet transmission time is

$$St_{x,k}(z) = z^{rts+cts+3sifs+ack} \sum_{r=1}^{Rg_{\max}} \frac{l_r}{L} z^{ld_{x,k,r}} \tag{2}$$

In case of collision of RTS packets, activity on the medium has the PGF of $Ct(z) = z^{rts+cts+sifs}$.

3.1. Distribution of vehicles

According to traffic flow theory [4], mean speed (v), flow, and density are related to each other as follows:

$$F = v\lambda_d \tag{3}$$

where F is the vehicle flow which corresponds to the number of vehicles that pass a fixed roadside point per unit time and λ_d is the vehicle density, that is, the number of vehicles per unit distance in one direction along the road segment.

Greenshield developed a model that captures the dependency between speed and density by assuming a linear relationship as follows [10]:

$$v = v_f(1 - \lambda_d/\lambda_{d,\text{jam}}) \tag{4}$$

where v_f is the free-flow speed corresponding to the maximum desired speed (usually taken as the road's speed limit). $\lambda_{d,\text{jam}}$ is the maximum allowable traffic density. Then, the maximum number of vehicles in each lane of road segment is denoted as $vh_{\max} = L\lambda_{d,\text{jam}}$.

Poisson and discrete version of Erlang-k distributions are used to model the distribution of the vehicles on the road segment. In Poisson distribution, the probability that there are n vehicles in each lane of the road segment is given by

$$Pois(n) = \frac{e^{-L\lambda_d} \frac{(L\lambda_d)^n}{n!}}{\sum_{i=0}^{vh_{\max}} e^{-L\lambda_d} \frac{(L\lambda_d)^i}{i!}} \tag{5}$$

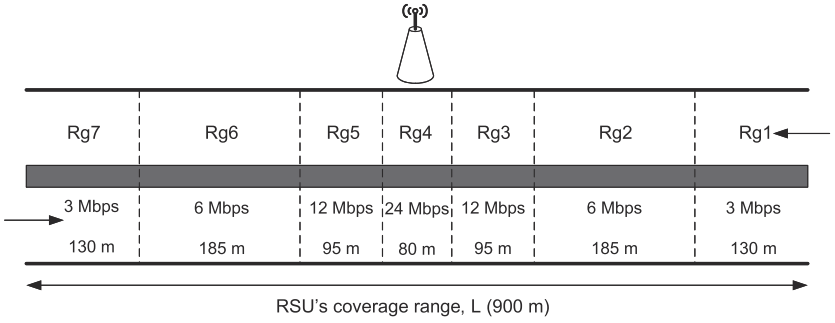

Figure 3. Road segment. RSU, roadside unit.

The probability distribution of the vehicles in discrete version of Erlang-k distribution is given by

$$Erl_k(n) = \frac{\frac{(k\mu)^k n^{k-1} e^{-k\mu n}}{(k-1)!}}{\sum_{i=0}^{vh_{\max}} \frac{(k\mu)^k i^{k-1} e^{-k\mu i}}{(k-1)!}} \tag{6}$$

where $\mu = \frac{1}{L\lambda_d}$ and k is stage parameter of Erlang-k distribution.

3.2. Model of control channel/service channel switching

Let us consider Figure 2 and denote the durations in backoff slots of CCH, SCH, and guard periods as *cch*, *sch*, and *grd*, respectively. Sum of channel time durations and guard intervals (in slots) must be constant and equal to the synchronization interval $si = cch + sch + 2grd$.

In order to model the impact of channel switching on the duration of backoff, we focus on the backoff process belonging to data combination d and traffic class k started in a random slot in one CCH (SCH). If the backoff process has started relatively close to the end of channel time and if it is long, because of collisions, it will exceed the current channel time and, consequently, it will have to be continued in the following CCH (SCH) time. This will effectively extend the backoff time and the entire frame service time. In order to evaluate the impact of this extension, we need to calculate its duration and average it over all slots in CCH (or SCH).

Furthermore, let us assume that we know the probability distribution of that backoff process in the form of the PGF

$$Bof_{c,d,k}(z) = \sum_{i=0}^{i_{\max}} b_{c,d,k,i} z^i$$

Then, the probability that the backoff process started in a given CCH interval will be completed in that same CCH is

$$Pl_{c,d,k}^{[1]} = \frac{1}{cch} \sum_{l=0}^{cch} \sum_{i=l}^{cch} b_{c,d,k,i-l} = \frac{1}{cch} \sum_{l=0}^{cch} \sum_{i=0}^{l} b_{c,d,k,i} \tag{7}$$

whereas the probability that the backoff process will be completed in κth CCH, $\kappa > 1$, is

$$Pl_{c,d,k}^{[\kappa]} = \frac{1}{cch} \sum_{l=0}^{cch} \sum_{i=0}^{l+(\kappa-1)cch} b_{c,d,k,i} \tag{8}$$

Consequently, the PGF for the duration of backoff process interleaved with durations of opposite channel can be expressed as

$$Bofe_{c,d,k}(z) = Bof_{c,d,k}(z) \left[Pl_{c,d,k}^{[1]} + \sum_{\kappa=1}^{\kappa_{\max}} \left(Pl_{c,d,k}^{[\kappa+1]} - Pl_{c,d,k}^{[\kappa]} \right) z^{\kappa(si-cch)} \right] \tag{9}$$

where $\kappa_{\max}$ is an integer selected as compromise between accuracy and complexity of this expression; in our calculations, we have found that the value $\kappa = 3$ gives satisfactory results.

Calculating extended backoff time for SCH follows a similar pattern.

A full model of IEEE 802.11p features can be found in our earlier work [3], from which we can calculate the desired performance indicators as follows.

3.3. Probability generating function for the frame service time

The probability that the node buffer is empty at arbitrary time is $\pi_{x,d,k,0} = 1 - \rho_{x,d,k}$ where $\rho_{x,d,k}$ denotes offered load from data combination d with class k in channel x. The entire Markov chain for AC_k is defined in [11]. The PGF for the backoff time for data combination d with data class AC_k in channel x becomes

$$\begin{aligned} Bof_{x,d,k}(z) = \sum_{r=1}^{Rg_{\max}} \frac{l_r}{L} \Bigg(& \sum_{i=1}^{m_{x,k}+1} \left(\prod_{j=0}^{i-1} B_{x,d,k,j}(z) \right) \cdot \left(1 - \delta_{k,r}\gamma_{x,d,k}\right)^{i-1} Ct(z)^{i-1} \delta_{k,r}\gamma_{x,d,k} \\ & + \sum_{i=m_{x,k}+1}^{R} \left(\prod_{j=0}^{m_{x,k}} B_{x,d,k,j}(z) \right) B_{x,d,k,m_{x,k}}(z)^{i-m_{x,k}} \cdot \left(1 - \delta_{k,r}\gamma_{x,d,k}\right)^{i} Ct(z)^{i} \delta_{k,r}\gamma_{x,d,k} \\ & + \left(\prod_{j=0}^{m_{x,k}} B_{x,d,k,j}(z) \right) B_{x,d,k,m_{x,k}}(z)^{R-m_{x,k}} \cdot \left(1 - \delta_{k,r}\gamma_{x,d,k}\right)^{R+1} Ct(z)^{R+1} \Bigg) \end{aligned} \tag{10}$$

where $B_{x,d,k,j}(z)$ is the PGF for the duration of the backoff phase j for data class k on channel x, as defined in [11].

When the buffer is found empty upon a successful packet transmission, the node can proactively undertake zeroth backoff, go to the idle state, and then attempt to transmit the next arriving packet upon waiting only for $AIFS_{x,k}$. However, if this attempt is not successful, the entire backoff process (beginning from phase 1) has to be performed; the PGF for the duration of this backoff process, $Bzof_{x,d,k}(s)$, is similar to the one in Equation (10):

$$Bzof_{x,d,k}(z) = \sum_{r=1}^{Rg_{\max}} \frac{l_r}{L} \left(\gamma_{x,d,k}\delta_{k,r} + \sum_{i=2}^{m_{x,k}+1} \left(\prod_{j=0}^{i-1} B_{x,d,k,j}(z) \right) \cdot \left(1-\delta_{k,r}\gamma_{x,t,k}\right)^{(i-1)} Ct(z)^{(i-1)} \delta_{k,r}\gamma_{x,t,k} \right.$$
$$+ \sum_{i=m_{x,k}+1}^{R} \left(\prod_{j=0}^{m_{x,k}} B_{x,d,k,j}(z) \right) B_{x,d,k,m_{x,k}}(z)^{i-m_{x,k}} \cdot \left(1-\delta_{k,r}\gamma_{x,d,k}\right)^{i} Ct(z)^{i} \delta_{k,r}\gamma_{x,d,k}$$
$$\left. + \left(\prod_{j=0}^{m_{x,k}} B_{x,d,k,j}(z) \right) B_{x,d,k,m_{x,k}}(z)^{R-m_{x,k}} \cdot \left(1-\delta_{k,r}\gamma_{x,d,k}\right)^{R+1} Ct(z)^{R+1} \right) \quad (11)$$

At this point, these expressions can be used to calculate extended backoff times $Bofe_{c,d,k}(z)$ and $Bzofe_{c,d,k}(z)$, as defined in [11].

If node's buffer is still empty after this backoff count, node enters idle state. The total idle state probability is calculated by finding the distance between two accesses by the same node. In order to obtain this result, we use Laplace–Stieltjes Transform (LST) of backoff time PGF, which is obtained as $Bofe^*_{x,d,k}(s) = Bofe_{x,d,k}(e^{-s})$. If we introduce probability of no frame arrivals during zeroth backoff on channel x as $v^0_{x,d,k,0}$ and LST of backoff process without the zeroth backoff phase as $Bzofe^*_{x,d,k}(s)$, the distance between two transmissions becomes

$$D^*_{x,d,k}(s) = \sum_{r=1}^{Rg_{\max}} \frac{l_r}{L} \left(St_{x,k}\left(e^{-s}\right) \left\{ \pi_{x,d,k,0} B_{x,d,k,0}\left(e^{-s}\right) v^0_{x,d,k,0} R^*_{x,k}(s) \left[\phi_i I^*_x(s) \left(\prod_{l=k+1}^{3} f_{x,l}^{A_{x,l,\max}\delta_{k,r}} \right.\right.\right.\right.$$
$$+ \left(1 - \prod_{l=k+1}^{3} f_{x,l}^{A_{x,l,\max}\delta_{k,r}} \right) Bofe^*_{x,d,k}(s) \Big) + \phi_a \left(f_{x,0}^{aifs_{x,k}\delta_{k,r}} \right.$$
$$\left.\left.\left.\left. + \left(1 - f_{x,0}^{aifs_{x,k}\delta_{k,r}}\right) Bofe^*_{x,d,k}(s) \right) \right] e^{-saifs_{x,k}} \right.$$
$$+ \pi_{x,d,k,0} B_{x,d,k,0}\left(e^{-s}\right) \left(1 - v^0_{x,d,k,0}\right) \left(\gamma_{x,d,k}\delta_{k,r} \right.$$
$$\left.\left.\left. + \left(1-\gamma_{x,d,k}\delta_{k,r}\right) Bzofe^*_{x,d,k}(s) \right) + \left(1-\pi_{x,d,k,0}\right) Bofe^*_{x,d,k}(s) \right\} \right) \quad (12)$$

Markov chain presents a random process with stationary distribution $y_{x,d,k,i,j,b}$, where $x \in (c,s)$, $d = 1,\ldots,d_x$, denotes node type; $k = 0,\ldots,3$ denotes the data class; $i = 0,\ldots,m_k$, denotes the index of the backoff phase; $j = 0,\ldots,W_{x,k,i}-1$, denotes the value of backoff counter; and $b = 0,\ldots,B_k$, denotes the value of the freezing counter.

In order to model behavior of node after the successful transmission, we need to note that the standard requires a vehicle to perform backoff with $W_{x,k,0}$ immediately after successful transmission even if the node's buffer is empty.

where $R^*_{x,k}(s) = \frac{\lambda_{x,k}}{\lambda_{x,k}+s}$ is the LST for exponential distribution of the residual frame inter-arrival time and $I^*_x(s)$ denotes LST of time needed to synchronize with the beginning of CCH or SCH period [11]. ϕ_a is the probability that the target channel is active when the node exits idle state and ϕ_i is the probability that the opposite channel (or guard time) is active. Then, the LST for the total active time between two successive access points (i.e., frame service time) is

$$
\begin{aligned}
Tt^{*}_{x,d,k}(s) = \sum_{r=1}^{Rg_{\max}} \frac{l_r}{L} \Bigg(St_{x,k}\left(e^{-s}\right) \Bigg\{ \pi_{x,d,k,0} B_{x,d,k,0}(e^{-s}) v^{0}_{x,d,k,0} \Bigg[\phi_i I^{*}_{x}(s) \Bigg(\prod_{l=k+1}^{3} f_{x,l}^{A_{x,l,\max}\delta_{k,r}} \\
+ \left(1 - \prod_{l=k+1}^{3} f_{x,l}^{A_{x,l,\max}\delta_{k,r}} \right) Bofe^{*}_{x,d,k}(s) \Bigg) + \phi_a \left(f_{x,0}^{aifs_{x,k}\delta_{k,r}} \right. \\
\left. + \left(1 - f_{x,0}^{aifs_{x,k}\delta_{k,r}}\right) Bofe^{*}_{x,d,k}(s) \right) \Bigg] e^{-saifs_{x,k}} \\
+ \pi_{x,d,k,0} B_{x,d,k,0}\left(e^{-s}\right) \left(1 - v^{0}_{x,d,k,0}\right) \left(\gamma_{x,d,k}\delta_{k,r} \right. \\
\left. + \left(1 - \gamma_{x,d,k}\delta_{k,r}\right) Bzofe^{*}_{x,d,k}(s)\right) + \left(1 - \pi_{x,d,k,0}\right) Bofe^{*}_{x,d,k}(s) \Bigg\} \Bigg)
\end{aligned}
\tag{13}
$$

3.4. Waiting time for AC_k in channel x

The PGF for the number of frame arrivals during frame service time is $A_{x,d,k}(z) = Tt^{*}_{x,d,k}(\lambda_{x,k}(1-z))$, and the PGF for the number of frames left after the departing frame in the node buffer is [12]

$$
\Pi_{x,d,k}(z) = \frac{\pi_{x,d,k,0}(1-z)A_{x,d,k}(z)}{A_{x,d,k}(z) - z} \tag{14}
$$

In order to calculate the response time, we observe that the number of frames left in the buffer after the departing frame is equal to the number of frames that arrived while the frame was buffered and serviced. If we denote the LST of the response time for AC_k in channel x as $W^{*}_{x,d,k}(s)$, the last statement can be written as $\Pi_{x,d,k}(z) = W^{*}_{x,d,k}(\lambda_{x,k} - z\lambda_{x,k}) Tt^{*}_{x,d,k}(\lambda_{x,k} - z\lambda_{x,k})$. Because of the PASTA property of M/G/1 systems, $\Pi_{x,d,k}(z)$ also presents probability distribution of buffer occupancy at arbitrary time. After substituting $s = \lambda_{x,k} - z\lambda_{x,k}$, we obtain the LST of the waiting time as $W^{*}_{x,d,k}(s) = \frac{s(1-\rho_{x,d,k})}{s-\lambda_{x,k}+\lambda_{x,k}Tt^{*}_{x,d,k}(s)}$, and its average value as $\overline{W_{n_{x,d,k}}} = \frac{\lambda_{x,k}\overline{Tt^{(2)}_{k}}}{2(1-\rho_{x,d,k})}$. The overall waiting time per lane can be calculated as

$$
E[\overline{W_{x,d,k}}] = \sum_{n=0}^{vh_{\max}} P(n)\overline{W_{n_{x,d,k}}} \tag{15}
$$

4. PERFORMANCE EVALUATION

We have evaluated the performance of a network with a single RSU with transmission range fixed to the value of $L = 900$ m, deployed on a bidirectional road segment. In order to investigate the effect of duty cycle on network operation, we have conducted a number of experiments with variable duty cycle and variable vehicle densities in a single contention domain of IEEE 802.11p. Poisson and discrete version of Erlang-k distributions with different k parameters are used for modeling the distribution of the vehicles on the road segment.

According to the distance of the vehicles from the RSU, data rate varies between 3 and 24 Mbps. Orthogonal frequency-division multiple access is chosen as the physical layer modulation mechanism with 40 μs as the duration of preamble and header transmission. Slot time is set to 16 μs, and the duration of *sifs* is two slot times. Bit error rate is set to $ber = 2 * 10^{-5}$. Frame size is set to 500 bytes. RTS/CTS scheme is used for medium access. We have assumed constant synchronization interval with duration $SI = 100$ ms and guard intervals of $gu = 5$ ms each. Duration of the CCH was varied as $(SI - 2gu)SO$, where duty cycle SO had values 0.3, 0.4, and 0.5, respectively. We have assumed that the traffic includes multiple data combinations and multiple data classes per combination, the details of which are shown in Tables III and IV.

Table III. Populations of vehicles and their data traffic running on the control and service channels.

Data combination	Data classes	Number of vehicles
1	*AC*1 and *AC*3	20% of vehicles
2	*AC*0 and *AC*2	20% of vehicles
3	*AC*0	60% of vehicles

Table IV. Data rates per data classes.

		Data rate (kbps)	
AC	Data type	CCH	SCH
*AC*1	Background	4	40
*AC*0	Best effort	4	40
*AC*2	Video	12	12
*AC*3	Voice	12	12

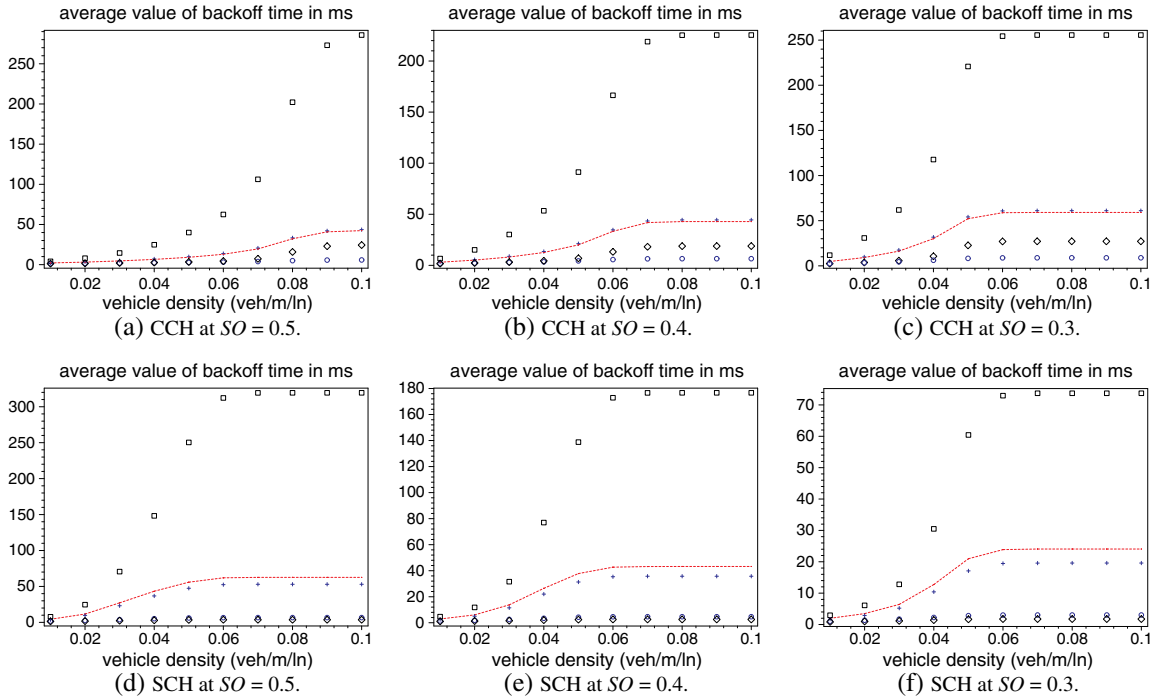

Figure 4. Average value of backoff time for Poisson distribution. Top row: control channel (CCH); bottom row: service channel (SCH).

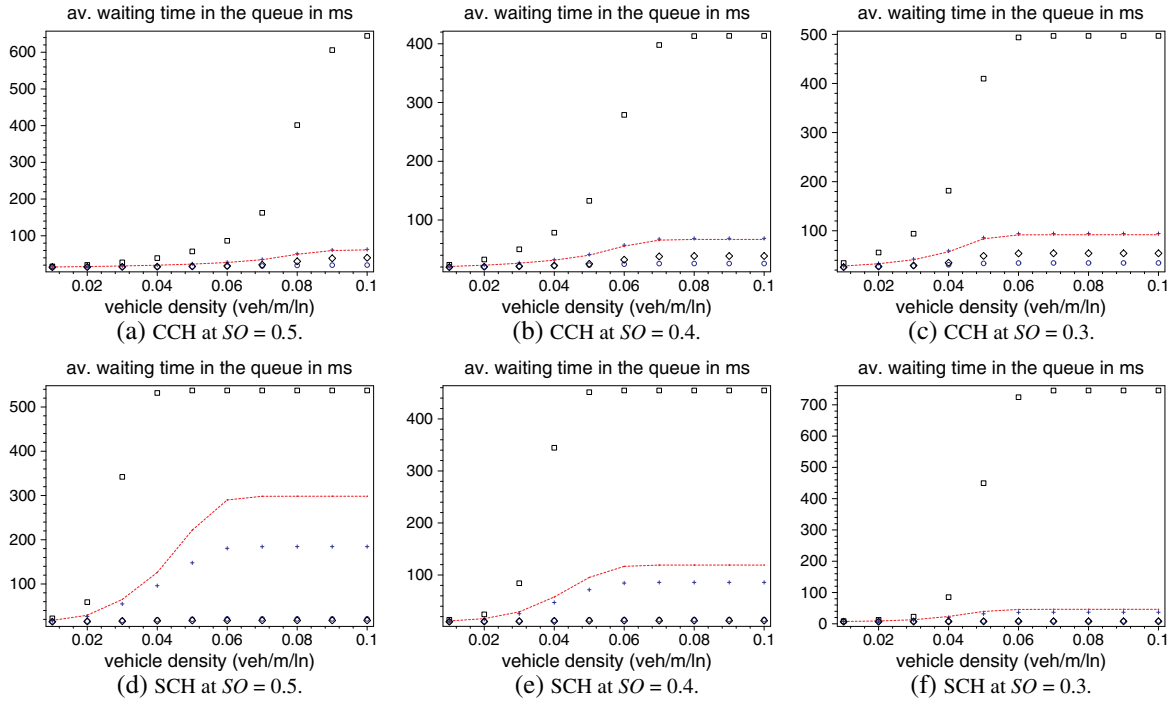

Figure 5. Average value of waiting time for Poisson distribution. Top row: control channel (CCH); bottom row: service channel (SCH).

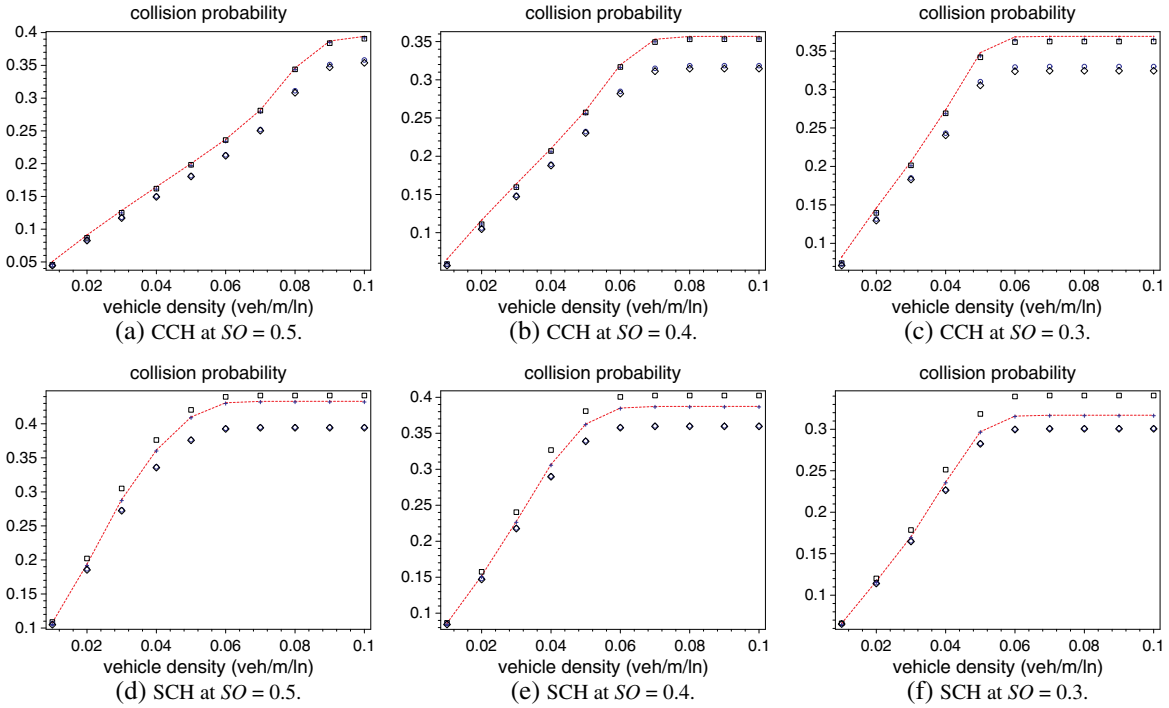

Figure 6. Average value of collision probability for Poisson distribution. Top row: control channel (CCH); bottom row: service channel (SCH).

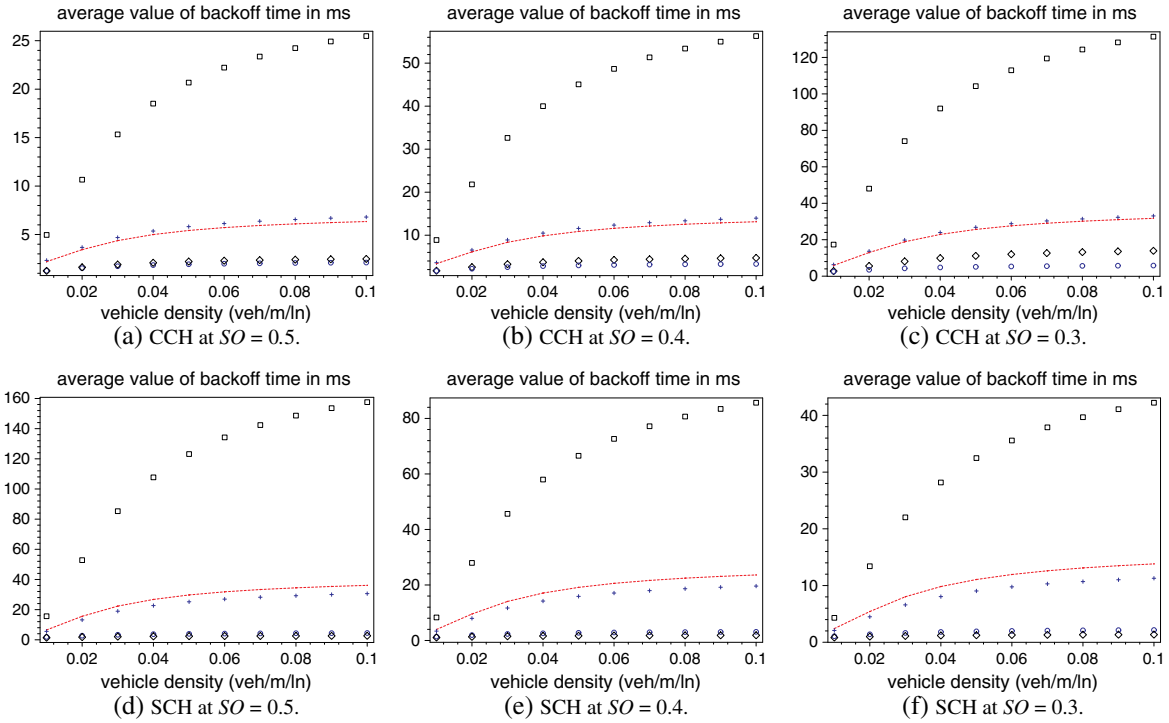

Figure 7. Average value of backoff time for Erlang-k distribution ($k = 1$). Top row: control channel (CCH); bottom row: service channel (SCH).

The maximum allowable traffic density, $\lambda_{d,\text{jam}}$, per lane is set to 0.1 veh/m (i.e., there is at most one vehicle per 10 m).

Using these parameter values, the analytical model was solved using MAPLE 13 [13]; the results for Poisson distribution are shown in Figures 4–6, which show the average backoff times, the average waiting times, and the collision probability, respectively. In all diagrams, the values for data classes of best effort ($AC1$), backgrounds ($AC0$s) in data combinations 2 and 3, video ($AC2$), and voice ($AC3$) are shown with boxes, crosses, dashed lines, circles, and diamonds, respectively.

The plots indicate that the default value of $SO = 0.5$ (in which case CCH and SCH are allocated equal time) leads to uneven performance between CCH and SCH traffic. For example, at $SO = 0.5$, the limit of useful operation for the lowest priority data class occurs at a vehicle density about 0.07 veh/m on CCH and around 0.03 veh/m on SCH. The reason for such behavior is that the difference in data frame arrival rates for $AC0$ and $AC1$ classes, both of which are higher in the SCH channel.

When the duty cycle is decreased to $SO = 0.4$, things begin to improve, but the balance is more or less obtained only at the duty cycle of $SO = 0.3$. In this case, approximately equal waiting times for both CCH and SCH traffic are achieved at the vehicle density of about 0.05 veh/m, which corresponds to about one vehicle per 20 m.

The results for Erlang-k distributions with $k = 1$ parameter are shown in Figures 7–9. From the figures, at $SO = 0.5$, the limit of useful operation for the lowest priority data class occurs at a vehicle density around 0.03 veh/m on SCH. There is no saturation on CCH at $SO = 0.5$ and 0.4. As the value of SO decreases to 0.3, saturation for the lowest priority data class occurs at a vehicle density about 0.06 veh/m on CCH and around 0.07 veh/m on SCH.

Figures 10–12 show the results for Erlang-k distributions with $k = 5$ parameter. At $SO = 0.5$, saturation for the lowest priority data class occurs at a vehicle density around 0.03 veh/m on SCH. There is no saturation on CCH at $SO = 0.5$ and 0.4. As the value of SO decreases to 0.3, saturation for the lowest priority data class occurs at a vehicle density about 0.04 veh/m on CCH, and around 0.05 veh/m on SCH.

Overall, as we increase the value of k parameters of Erlang-k distribution, the limit of useful operation for the lowest priority data class occurs earlier. It can be also observed that the results of Erlang-k distribution for higher k values are getting similar to the results of Poisson distribution.

Another observation that can be made from the diagrams is that higher data classes never experience networking saturation, unlike their lower-priority counterparts. However, they all do experience spatial saturation, which occurs at traffic density of about 0.1 veh/m per lane. In this case, the medium contention also increases, as indicated by the collision probability, which grows to a rather high values of around 0.3 (i.e., 30%) or so. While this value of spatial density is not very likely to occur at a high-speed segment of a highway, it may nevertheless easily be achieved in a traffic

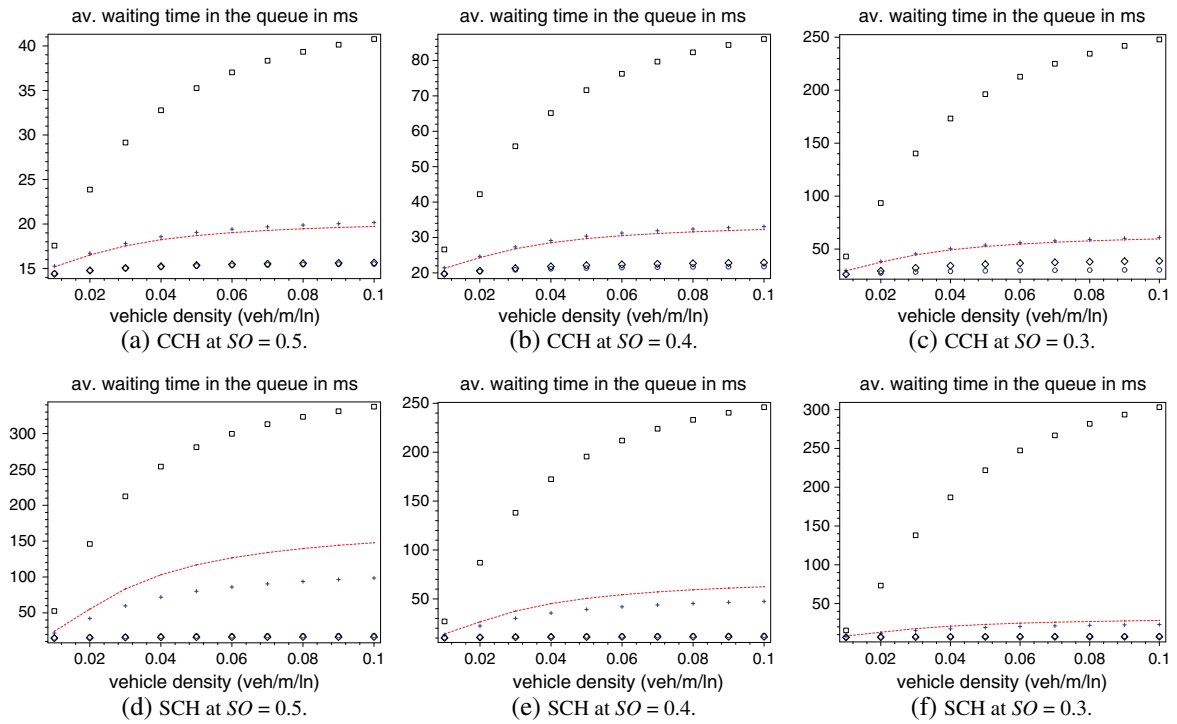

Figure 8. Average value of waiting time for Erlang-k distribution ($k = 1$). Top row: control channel (CCH); bottom row: service channel (SCH).

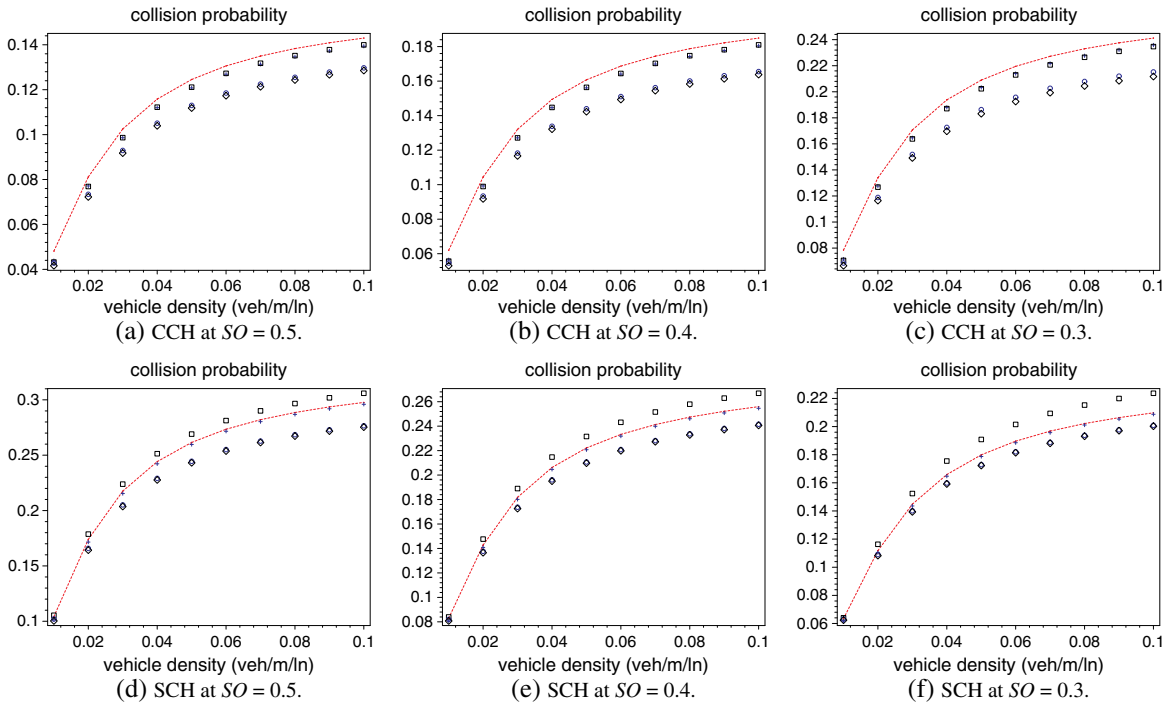

Figure 9. Average value of collision probability for Erlang-k distribution ($k = 1$). Top row: control channel (CCH); bottom row: service channel (SCH).

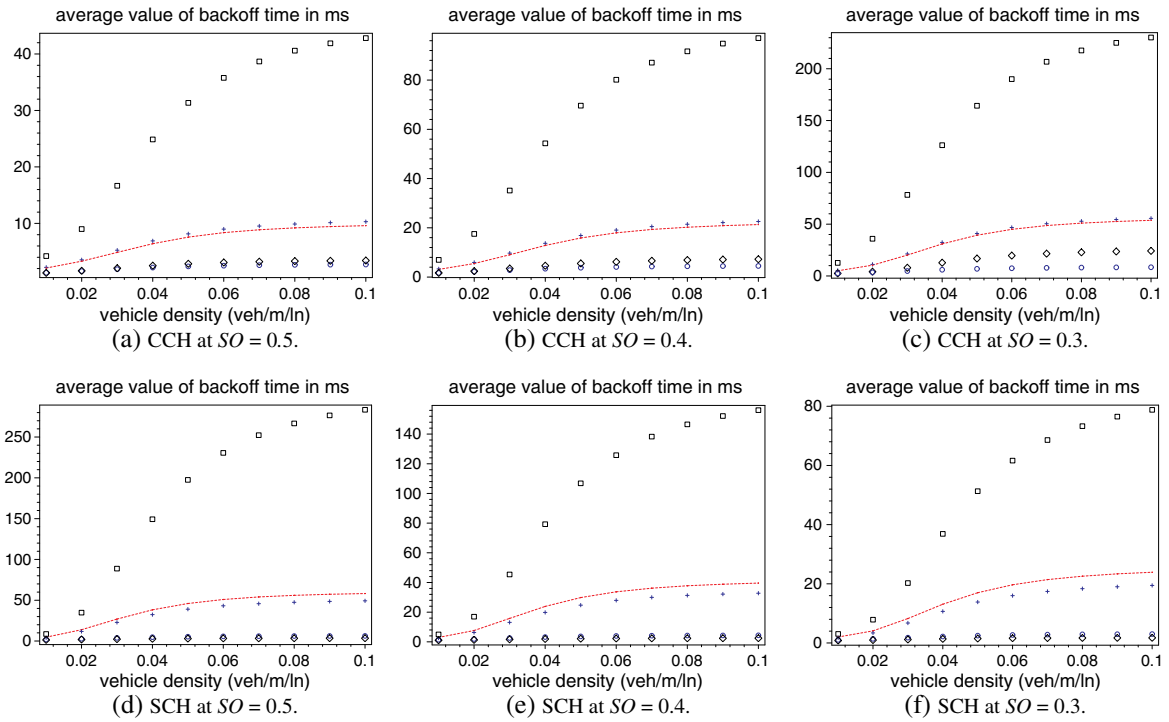

Figure 10. Average value of backoff time for Erlang-k distribution ($k = 5$). Top row: control channel (CCH); bottom row: service channel (SCH).

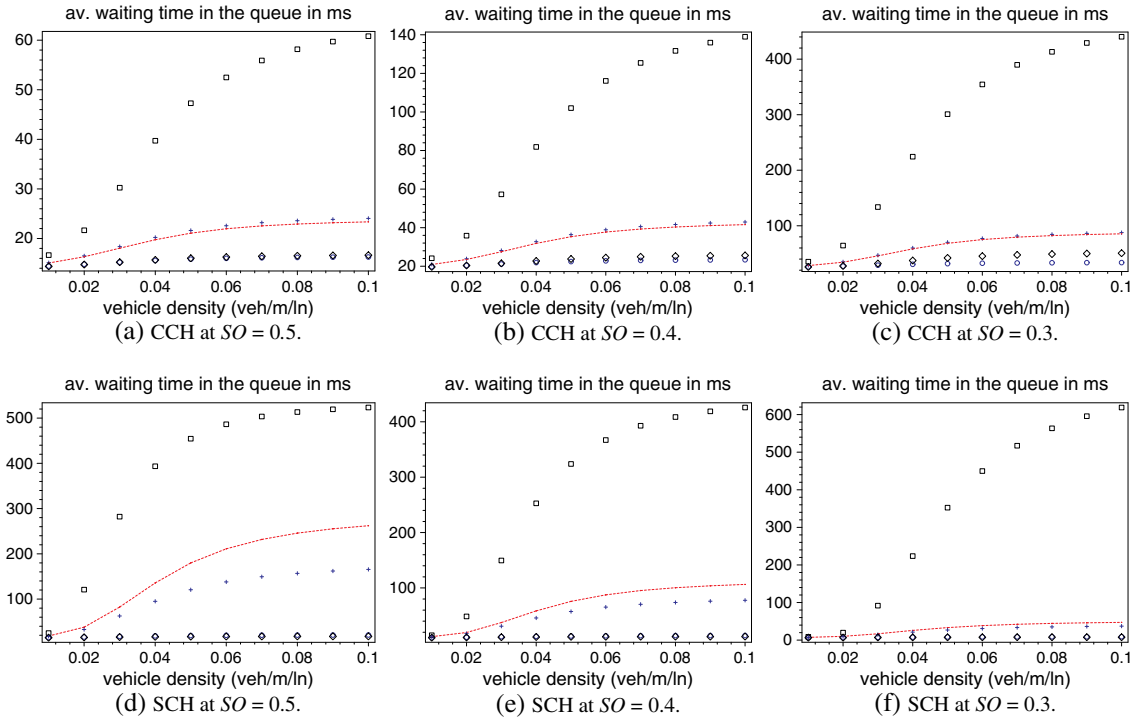

Figure 11. Average value of waiting time for Erlang-k distribution ($k = 5$). Top row: control channel (CCH); bottom row: service channel (SCH).

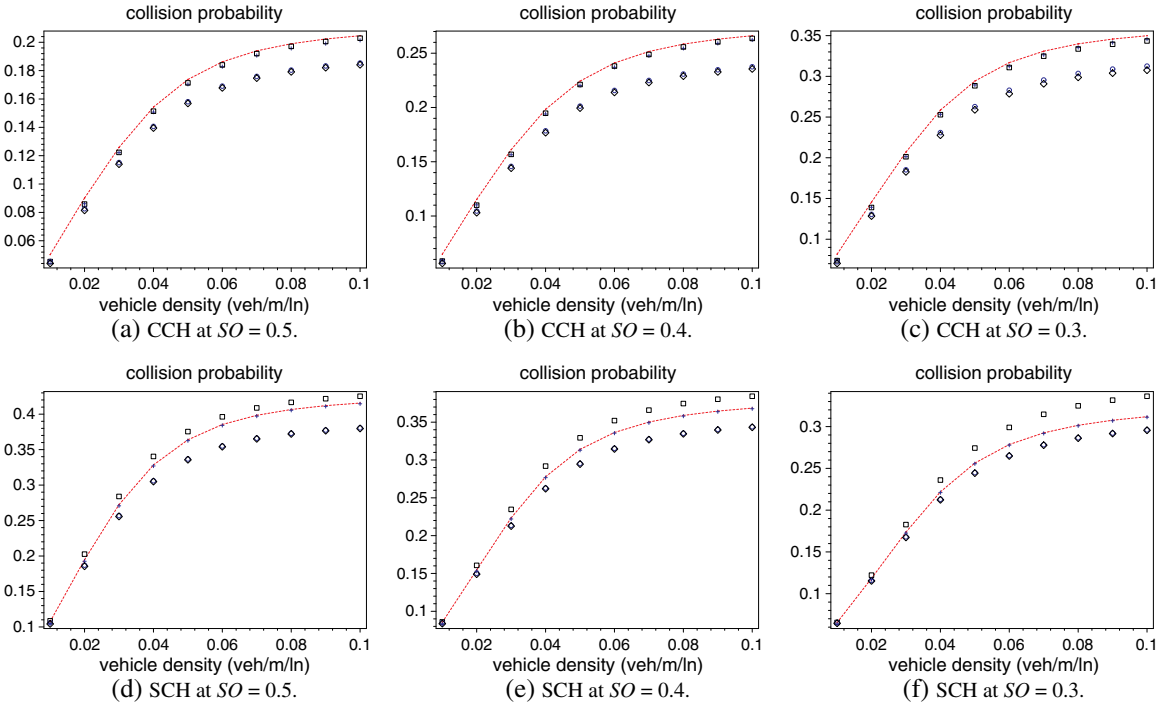

Figure 12. Average value of collision probability for Erlang-k distribution ($k = 5$). Top row: control channel (CCH); bottom row: service channel (SCH).

jam caused by, say, road works or an accident. In this case, some other measure must be taken to ensure unimpeded performance for traffic on both CCH and SCHs.

5. CONCLUSION

In this paper, we studied the effect of duty cycle—that is, time allocation between CCH and SCHs in an IEEE 802.11p-based network—needed to balance the capacity of those channels. The balance is needed in order to maximize the revenues from services (such as infotainment) provided on the SCH while not compromising safety, which is accomplished through high-priority messages on the CCH. Our results indicate that the default duty cycle value of $SO = 0.5$ leads to unsatisfactory performance on the SCH; much more balanced results are obtained when the SCH is allocated more time, for example, at a duty cycle value of about $SO = 0.3$. However, more work is needed to investigate this behavior and, possibly, design an adaptive scheme that will try to obtain the desired trade-off in different vehicular networking scenarios.

We also compared the effect of different distributions, such as Poisson and Erlang-k, in our model. We used different k parameters to evaluate the Erlang-k distribution. As we increase the value of k parameters of Erlang-k distribution, saturation of the lowest priority data class occurs earlier. The results of Erlang-k distribution for higher k values are getting similar to the results of Poisson distribution.

REFERENCES

1. *IEEE Trial-use Standard for Wireless Access in Vehicular Environments (WAVE)—Multi-channel Operation*. IEEE: New York, NY , IEEE Std 1609.4, 2007.
2. Öztürk S, Mišić J. On non-saturation regime in ieee 802.11p-based VANET with mobile nodes, In *Proc. IEEE PIMRC*, Toronto, ON, 2011; 740–744.
3. Öztürk S, Mišic J, B. Mišic V. Reaching spatial or networking saturation in vanet. *EURASIP Journal on Wireless Communications and Networking* 2011; **2011**(1): 174.
4. Roess RP, Prassas ES, McShane WR. *Traffic Engineering*, 3rd ed. Pearson Prentice Hall: Upper Saddle River, NJ, 2004.
5. Tan WL, Lau WC, Yue O. Modeling resource sharing for a road-side access point supporting drive-thru internet, In *ACM VANET'09*, Beijing, China, September 2009; 33–42.
6. Zhuang Y, Viswanathan V, Pan J, Cai L. Upload capacity analysis for drive-thru internet. *Techical Report*, University of Waterloo, ON, 2010. Available from: https://129.97.58.88/ojs-2.2/index.php/pptvt/article/view/619/213 [Accessed on September 2012].
7. Bruno R, Conti M. Throughput and fairness analysis of 802.11-based vehicle-to-infrastructure data transfers, In *IEEE MASS 2011*, Valencia, Spain, October 2011; 232–241.
8. Luan TH, Ling X, Shen XS. MAC in motion: impact of mobility on the MAC of drive-thru internet. *IEEE Transactions on Mobile Computing* 2012; **11**: 305–319.
9. Zhang G, Wang Y, Wei H, Chen Y. Examining headway distribution models using urban freeway loop event data. *Transactions Research Record* 2007; **1999**: 141–149.
10. Fricker JD, Whitford RK. *Fundamentals of Transportation Engineering: a Multimodal Systems Approach*. Prentice Hall, 2004.
11. Mišić J, Badawy G, Mišić VB. Performance characterization for IEEE 802.11p network with single channel devices. *IEEE Transactions on Vehicular Technology* 2011; **60**(4): 1775–1787.
12. Takagi H. *Queueing Analysis*, vol. 1: Vacation and Priority Systems. North-Holland: Amsterdam, The Netherlands, 1991.
13. *Maple 13*. Maplesoft, a division of Waterloo Maple, Inc.: Waterloo, ON, 2009.

AUTHORS' BIOGRAPHIES

Serkan Ozturk received his BSc degree in Computer Engineering from Karadeniz Technical University, Trabzon, Turkey, in 1999, MSc degree in Electronic Engineering in 2002, and PhD degree in Electronic Engineering from Erciyes University, Kayseri, Turkey, in 2009. He conducted a post-doctoral research in the Department of Computer Science at Ryerson University, Toronto, Canada, between 2010 and 2011. He is currently working as an assistant professor in the Department of Computer Engineering at the Erciyes University. His research interests include wireless communication, information security, and image processing.

Jelena Mišić is a professor of Computer Science at Ryerson University in Toronto, Ontario, Canada. She has published more than 90 papers in archival journals and more than 120 papers at international conferences in the areas of wireless networks, in particular wireless network protocols, performance evaluation, and security. She serves on editorial boards of the IEEE Transactions on Vehicular Technology, Computer Networks and Ad hoc Networks, Wiley Security and Communication Networks, Ad Hoc & Sensor Wireless Networks, Int. Journal of Sensor Networks, and Int. Journal of Telemedicine and Applications journals. She is a senior member of the IEEE.

Vojislav B. Mišić is a professor of Computer Science at Ryerson University in Toronto, Ontario, Canada. He received his PhD in Computer Science from the University of Belgrade, Serbia, in 1993. His research interests include performance evaluation of wireless networks and systems and software engineering. He has authored or co-authored six books, 18 book chapters, and close to 200 papers in archival journals and at prestigious international conferences. He serves on the editorial boards of the IEEE Transactions on Parallel and Distributed Systems, Ad Hoc Networks, Peer-to-Peer Networks and Applications, Int. Journal of Parallel, Emergent and Distributed Systems, and Journal of Computer Systems, Communications and Networking. He is a senior member of the IEEE and a member of ACM and AIS.